

Coronal Mass Ejections: A journey from its origin to its transport in the interplanetary medium

Dr. Andrea Inés Borgazzi

Geophysics Institute UNAM

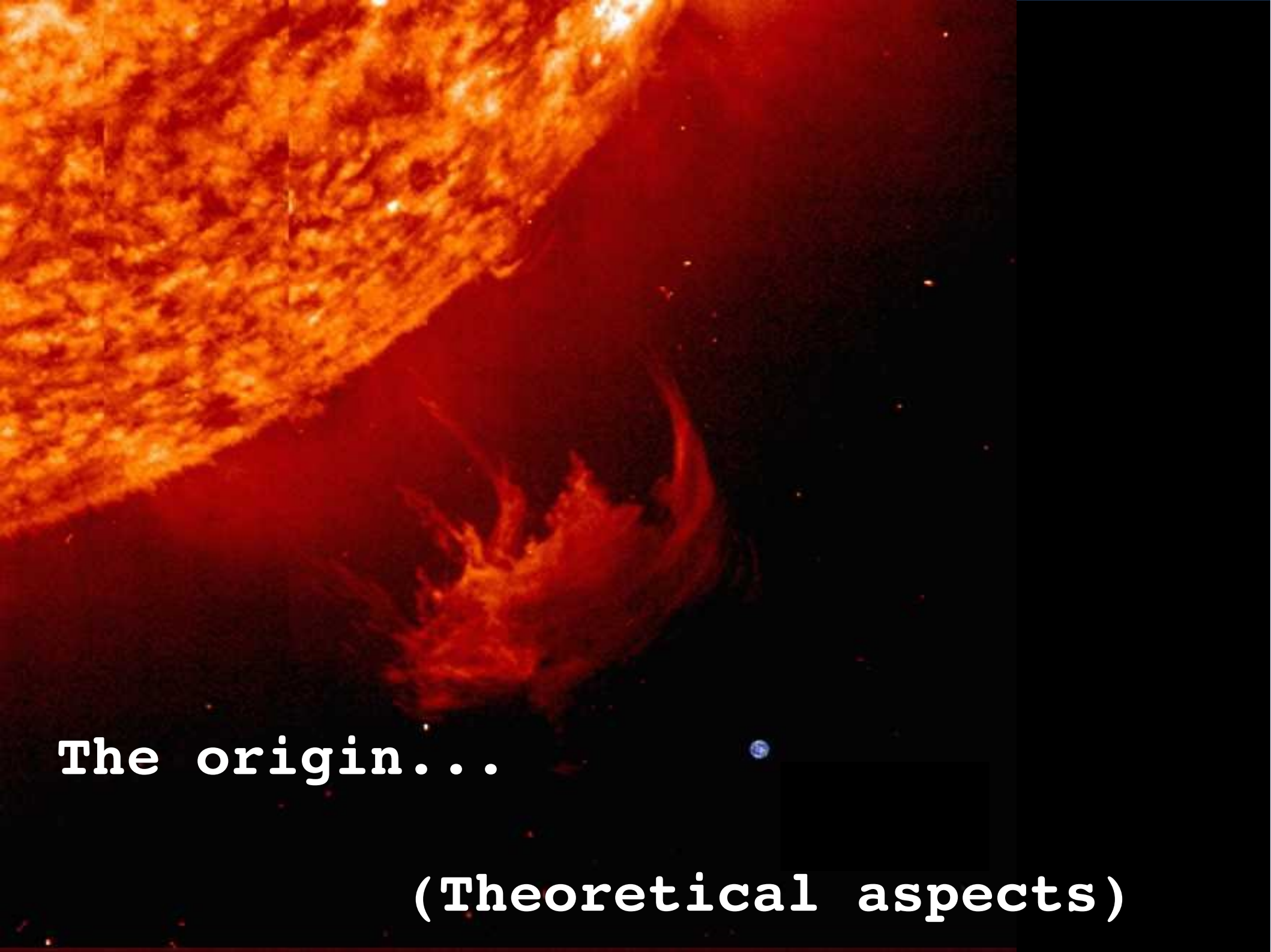
Invited overview talk ISEST/MiniMax 2015 Workshop
andrea@geofisica.unam.mx



Abstract

In the description of the dynamic behavior of CMEs and ICMEs many attempts have been done to quantify the interaction with the solar wind. From the theoretical point of view different kinds of models have been proposed to explain its origin and propagation in the interplanetary medium since its discovery until today.

This overview talk aims to describe these CME models, taking into account the measurable physical parameters that we have today.



The origin...

(Theoretical aspects)

- Flux rope
- Flux cancellation
- Break-out
- Flux injection
- Shearing motions
- Emerging flux triggering
- Tether-Cutting
- Tether Straining
- Instabilities Catastrophe
- Torus instability
- Hybrid mechanisms
- Others mechanism

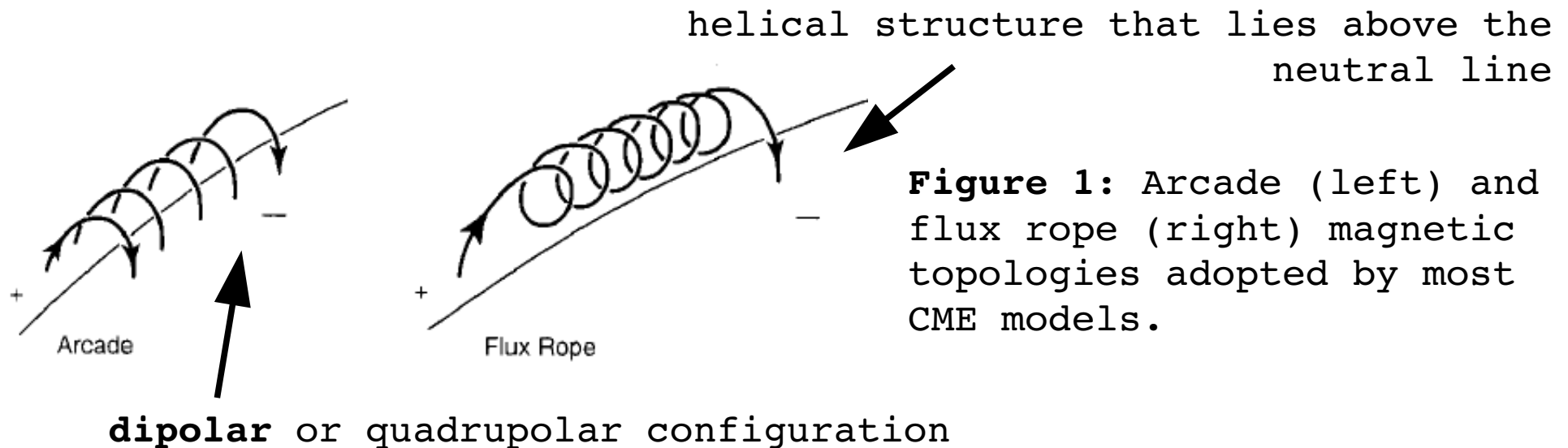
'Which of the proposed models is correct?. Perhaps none is, or perhaps several are'... (Klimchuk, 2001).

'Several mechanisms can explain the onset of CMEs. The observations also teach us that various mechanisms proposed by the theoretical models can exist or co-exist'... Schmieder (2015).

begin

It is always interesting for researchers to know what kind of structures have the potential to erupt as a CME.

In most models, the **pre-eruption magnetic field** has one of the two basic topologies illustrated in **Figure 1**.



For CMEs, the progenitor ———▶ strongly twisted or sheared magnetic structure ———▶ has stored a lot of nonpotential energy.

The structure should have a potential to erupt while being kept in a metastable equilibrium (Chen, 2012)

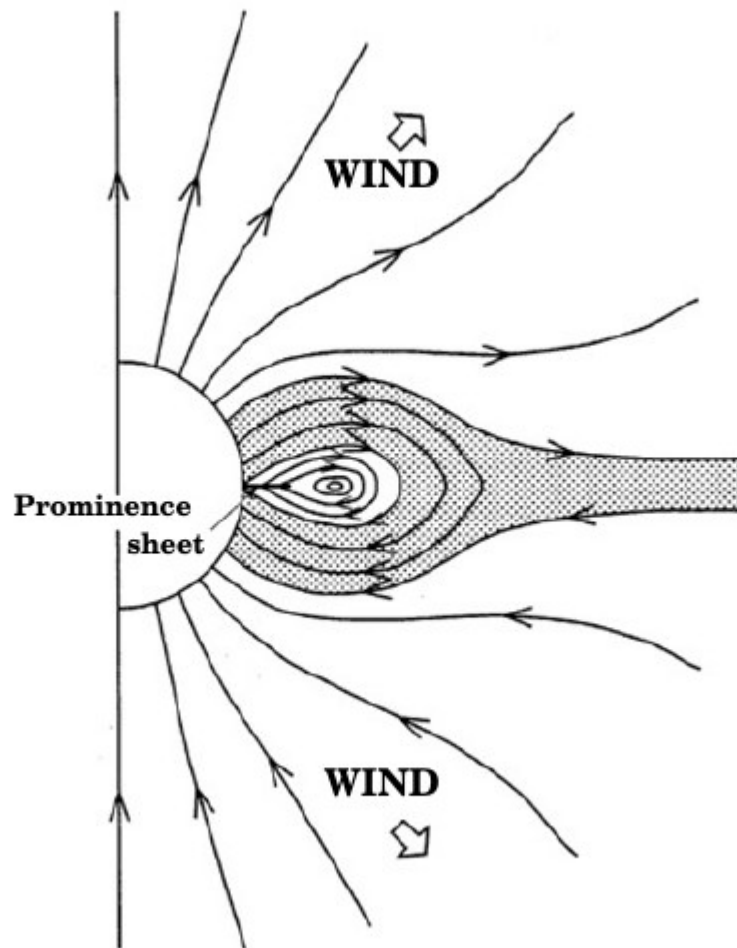


Figure 2: The flux rope model for the CME progenitor, where the shaded area corresponds to the dome of a helmet streamer surrounding a cavity in the middle, and a prominence is located at the bottom of the flux rope (from Low and Hundhausen, 1995).

We define the progenitor as the unstable or metastable coronal structure that would be the source of a CME.

The **precursors for CMEs** found in the past decades can be summarized as follows:

- (1) Helmet streamer swelling and/or slow rise of prominences.
- (2) Reconnection-favored emerging flux.
- (3) SXR brightenings.
- (4) Radio noise storms.
- (5) Type III radio burst group.
- (6) Filament darkening and widening.
- (7) Long-term filament/prominence oscillations.
- (8) Outward-moving blobs near the edge of streamers.

Magnetic flux —► **emerge from the subsurface, colliding with the pre-existing field** —► **electric current layers or even current sheets.**

Photospheric motions (various length scales) —► **drag the footpoints of all the magnetic field lines** to move in both organized and random ways, **building up a highly stressed coronal magnetic field** (Forbes, 2006).

We need energy → What is the source of this energy?

Could be that energy passes through the solar surface from below the corona during the time of an eruption.

'is likely to be stored in the corona before the eruption begins'

As $\beta = 8\pi P / B^2 \ll 1$ → in the corona → energy is probably **magnetic**.

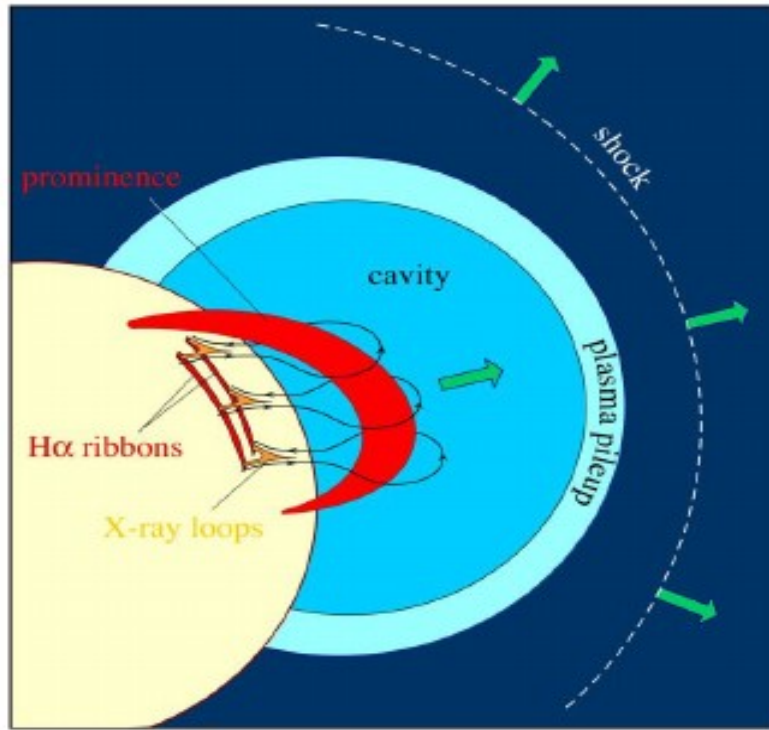
Only a part of the magnetic energy associated with electric currents, "free magnetic energy," is available to be converted to other forms.

Energy cannot be extracted from a current-free potential field → the field must be stressed.

Energy_(pre-eruption-coronal-fields) is \geq gravitational and kinetic energies CME [e.g., Klimchuk and Sturrock, 1992; Wolfson, 1993]

The energy problem is not so easily solved

How we can open the field to the extent required by observations and at the same time decrease its energy by a sufficient amount to power the mass motions?



CME Initiation ...the
onset Klimchuk (2001)

...identify the essential physics
involved in the CME problem, and to
distinguish the various types of models
in terms of their most basic physical
differences...

Models which answer this
question are...

FIRST

"storage and release models"

STORAGE: refers to the slow buildup of magnetic free energy from the gradual stressing of the field by footpoint motions or mass accumulation. It is a phase of quasistatic evolution.

RELEASE: refers to the highly dynamic phase when rapid energy conversion and eruption take place.

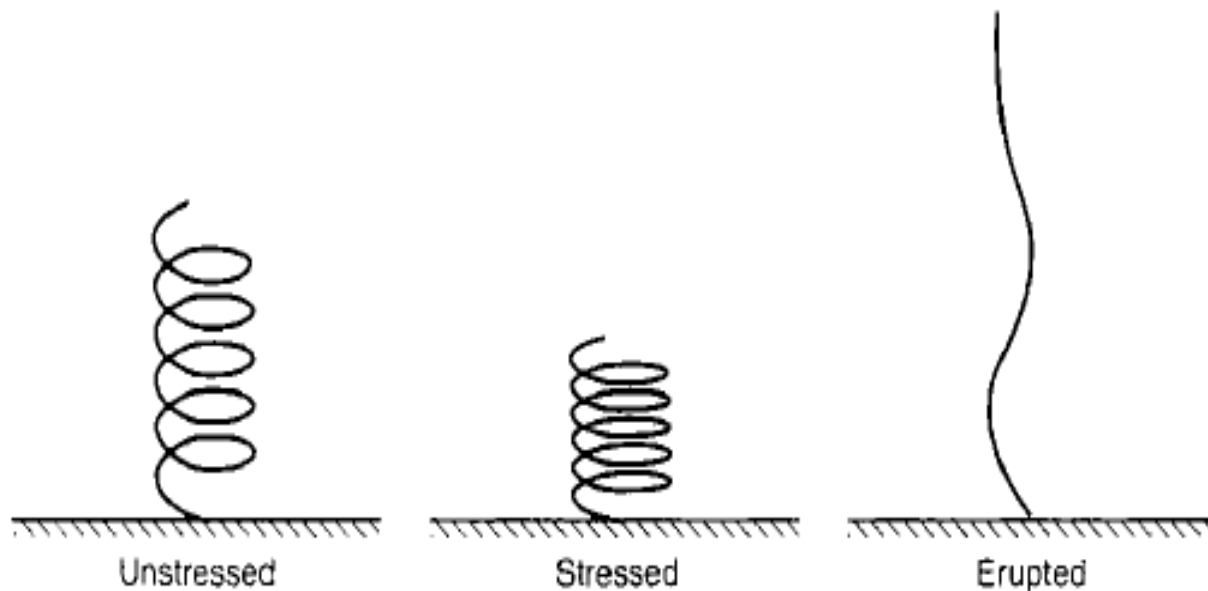


Figure 3:

Spring analogue.
The magnetic field
when it is unstressed
(potential), stressed
(current-carrying),
and erupted (also
current-carrying).

In **storage** and **release** models, the system evolves slowly from the unstressed to stressed states, and then rapidly from the stressed to erupted states.

SECOND

"directly driven models"

These models bypass the intermediate stressed state and go directly from the unstressed state to the erupted state.

- ◆ The flux rope could be formed from a part of the magnetic arcade (Mikic and Linker, 1994).
- ◆ For some models **the existence** of a flux rope **is apparently not necessary** (Delannée and Aulanier, 1999; Sun et al., 2014).

Currently, **popular** CME-triggering mechanisms are:

the tether-cutting (Moore et al., 2001),

the break out (Antiochos, DeVore, and Klimchuk, 1999; Jacobs et al., 2009),

the torus instability (Kliem and Török, 2006; Kliem et al., 2010; Török and Kliem, 2005).

Numerical simulations are very helpful for testing the role of the different parameters involved in CME triggers.

The analysis of observations is essential to constrain and test theoretical models

(2) Shearing motions

The shearing motion is indeed one important way for the corona to build up free energy (Low, 1977)

(3) Magnetic breakout model

Antiochos et al. (1999) proposed the so-called magnetic breakout model.

The initial magnetic configuration consists of a quadrupolar topology, with a null point being above the central flux system.

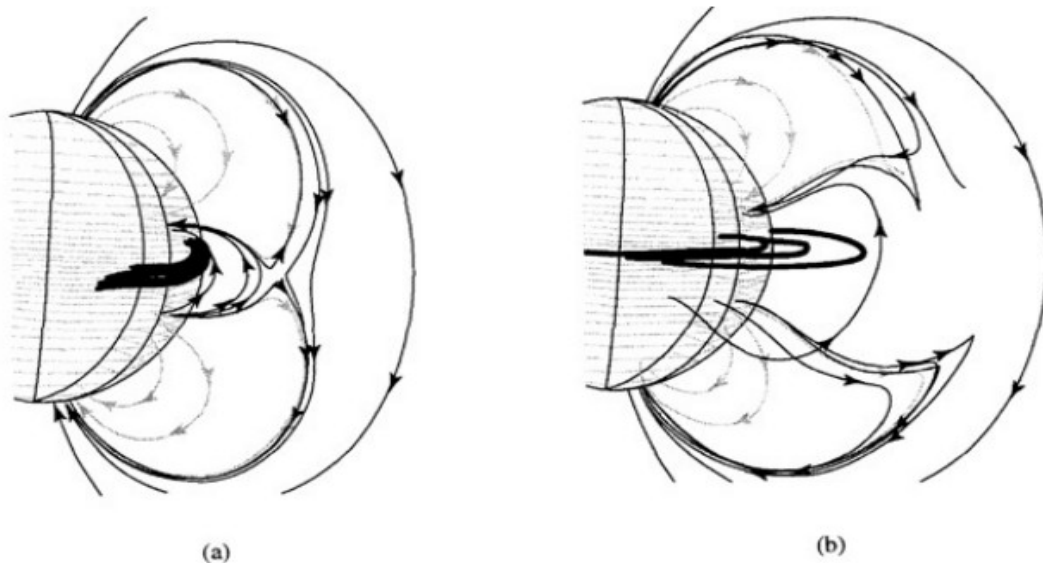


Figure 8: The evolution of the magnetic field in the breakout model, showing the reconnection above the central flux system removes the constraint over the core field (thick lines), and results in the final eruption (adapted from Antiochos et al., 1999).

The first **evidence** supporting the **breakout model** was presented by Aulanier et al. (2000) → **null point** above the source region in the extrapolated coronal magnetic field.

(4) Emerging flux triggering mechanism

Using → magnetograms before CME eruptions.

Chen (1989, 1997, 2000) → many CMEs are preceded by emerging flux that possesses polarity orientation **favorable for magnetic reconnection.**

The **flux injection triggering** mechanism was **criticized** in the sense that the flux injection **process would induce too large surface motions** that **have not been observed** (e.g., Forbes, 2000; Schuck, 2010).

(6) Instability and catastrophe-related triggering mechanisms

(a) Kink instability: Sakurai (1976) numerically analyzed the development of the **kink instability** of a **twisted flux tube**.

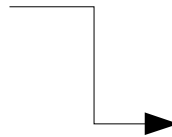
The kink instability can explain the observed height-time profile of an erupting filament

(b) Torus instability: A current ring is unstable against expansion if the external potential field decays sufficiently fast, e.g., $\partial \ln B / \partial \ln r > 3/2$ (Bateman, 1978)

Was called torus instability by Kliem and Torok (2006)

(7) Hybrid mechanisms

van Tend and Kuperus (1978)
Priest and Forbes (1990)



Constructed a model to study the equilibrium of a line current filament in the background coronal magnetic field.

It was found that as the **filament current or twist increases to a critical value**

catastrophe takes place

(8) Other mechanisms

Besides the above-mentioned triggering models, there are some other mechanisms that have not been investigated extensively and quantitatively.

(a) Mass drainage:

The filaments are supported by the Lorentz force against gravity. If a part of filament material drains down to the chromosphere, the filament would lose its equilibrium under the excess Lorentz force

(TandbergHanssen, 1974; Low, 2001), Fan and Low (2003), Wu et al. (2004), (Zhou et al., 2006).

(b) Sympathetic effect:

Moreton waves and/or EIT waves generated by some CME events might trigger the oscillation

(Eto et al., 2002; Okamoto et al., 2004) (Ballester, 2006).

(c) Solar wind:

It is possible that the CME source region might be pulled by the solar wind.

In this sense, the combinative study on the internal cause, the free energy, and the external cause, a suitable trigger, becomes crucial.

The analysis of observations **is essential to constrain** and test theoretical models.

open questions concerning the CME triggering mechanisms that are still not answered by the theoretical models alone

Most of **MHD numerical CME models** involve a flux rope in an active region that commonly is **represented by a bipolar field**

(Wu et al., 2004; Török and Kliem, 2005; Shiota et al., 2010; Lugaz and Roussev, 2011).

This type of models does not bring any information on flux rope formation

Some CME **initiation models can be tested by applying a topological analysis** to observations since models require the presence and activation of some specific topological features.

What about the pair CME-flare?

Flares and CMEs \longrightarrow can be considered as different manifestations of the same physical process.

The conversion of magnetic free energy to radiative and kinetic energies, respectively (Harrison, 1995).

Relationship between flares, filament eruptions, and CMEs is:
statistics

(Harrison, 1995; Zhang et al., 2001; Subramanian and Dere, 2001; Vrřnak, Sudar, and Ruždjak, 2005; Marić et al., 2007; Bein et al., 2012).

Up to **25 %** of CMEs are only associated with filament eruptions, without a flare detected by GOES (Bein et al., 2012)

It is nevertheless frequently observed that a CME associated with a flare is also associated with a filament eruption (**70 %**)

However, apparently, they are not in a cause effect relationship, as demonstrated by Zhang et al. (2001)

- CMEs are associated with the **so-called eruptive flares**.
- Opposed the: **so-called confined flares** —→ flares that **are not** associated with CMEs (Priest, 1981; see also, e.g., Schmieder et al., 1997; Guo et al., 2012; Dalmasse et al., 2014).

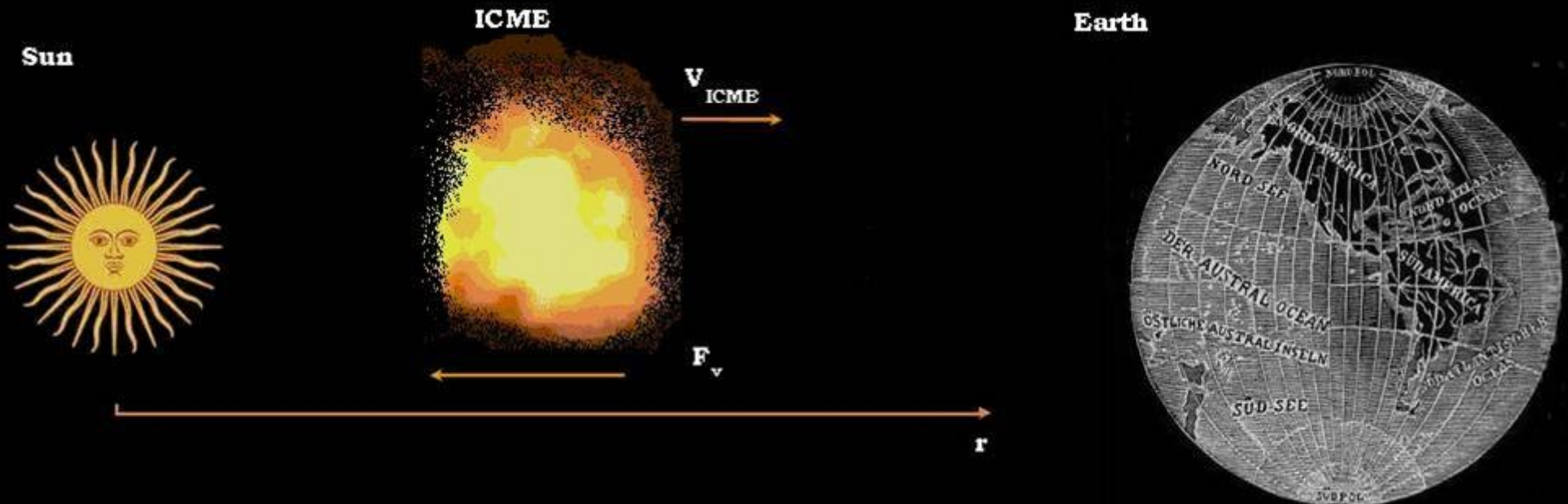
Flares without CMEs —→ have a **higher temperature**.

The magnetic energy —→ **concentrated in the heating of the plasma**,
CME-associated flares —→ **accelerating the ejecta** (Yashiro et al., 2006).

Past 50 years, flare and CME models —→ progressed from the **standard two-dimensional (2D) CSHKP model** (Carmichael, 1964; Sturrock, 1966; Hirayama, 1974; Kopp and Pneuman, 1976).

THE TRANSPORT...

(theoretical aspects)



CME Propagation

(Statement of Problem)

After the formation  CME propagates (IM)  by assimilation (MIR) in the outer heliosphere  loses identity.

Analytical approach  specify the equations (spatially varying solar wind velocity, deceleration, and deformation forces)

Ordinary differential equations determine the position of the ICME and its geometry as a function of time

MHD simulations  the fields are specified at every point of a simulation grid

(not at the center of mass of an ICME as in the analytic formulation)

Theoretical models - Transport

<u>CMEs</u>	acceleration	velocity	Size - rate of expansion 1 AU
24 Zhang et al. (2005)	200 m/s ² - 40 min - 0.82 RS		
28 Gopalswamy et al. (2000)		124km/s-1,056km/s	
Hu and Sonnerup, (2002)			0.2 - 0.25 AU

Empirical relation (v)	Empirical relation (a)	ratio of the major to minor axes
$V_{EXP}[km/s] = 0.266 V_{LE}[km/s] - 70.61$	$a[m/s^2] = 1.41 - 0.0035 u[km/s]$	less than 2 (Hu and Sonnerup, 2002) loser to 4 (Mulligan and Russell, 2001)

Owens et al. (2005). Rate at which the ICME radius is increasing

Gopalswamy et al. (2001)

Virtual Mass

Is a concept from **hydrodynamics** that allows one to express, by **an appropriate increase in the mass of the body, the force needed to move the ambient medium out of the way as the body accelerates.**

Acceleration and Virtual Mass

Recall that observed accelerations of CMEs in the inner corona vary from a few m/s^2 up to $\sim 1000 \text{ m/s}^2$.

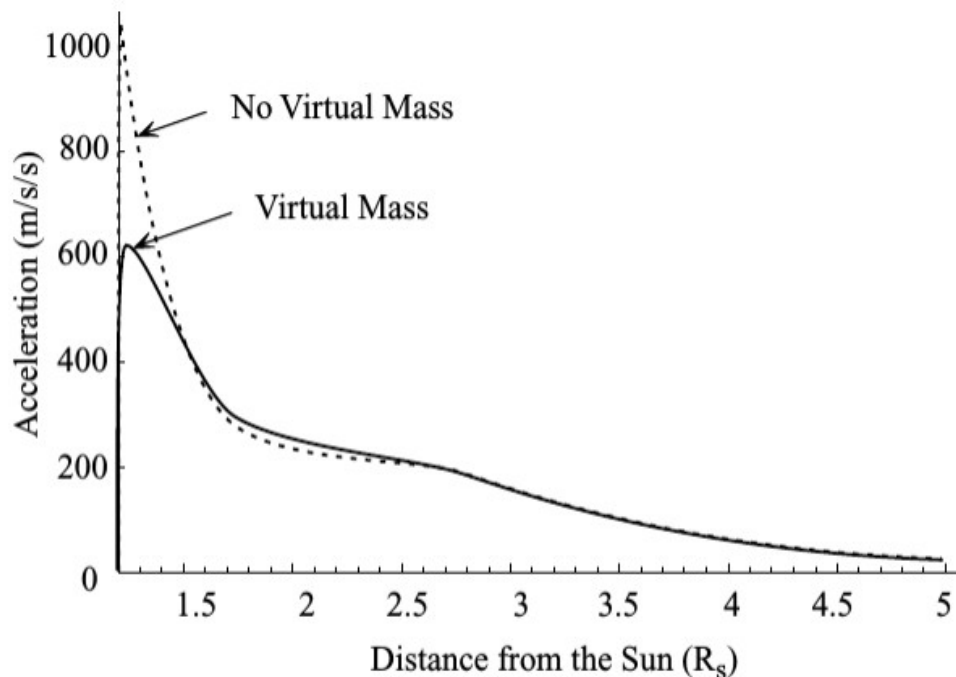


Figure 14: Computed accelerations in the inner corona for the cases of virtual mass and no virtual mass using the equations that generated the Variable C_D .

virtual mass —→ the equation brings the peak acceleration into the observed range

but after —→ virtual mass has little effect on acceleration

Beyond about 1.5 Rs, **ambient density**, which makes up virtual mass, is relatively **small**

Some Conclusions

The **transport properties** of fast —→ by expansion under magnetic over-pressure

Drag appears to be weak near the Sun (possibly because of magnetic suppression of a low-pressure wake) but more-or-less normal farther out

using

The basic information \longrightarrow CME kinematics

Distance-time measurements of a particular element of the eruption

used to determine the acceleration time-profile $a(t)$ or $a(r)$

(Zhang et al., 2001, 2004; Gallagher et al., 2003; Maricic et al., 2004)

We know the net force acting on the CME

The driving force

net acceleration \longrightarrow $a = a_L - g + a_d$

- a_L Lorentz-force acceleration.
- g is the acceleration of gravity.
- a_d is the 'aerodynamic' drag (Cargill et al., 1996; Vrsnak et al., 2004)

More than **5000** CMEs measured in the distance range **2 – 30** solar radii is investigated in Vrsnak et al. (2004)

Anticorrelation between a and v exist

represented by:

$$a = -k_1 (v - v_0), \quad v_0 = 400 \text{ kms}^{-1}$$

(most of CMEs faster than 400 kms^{-1} decelerate, whereas slower ones generally accelerate)

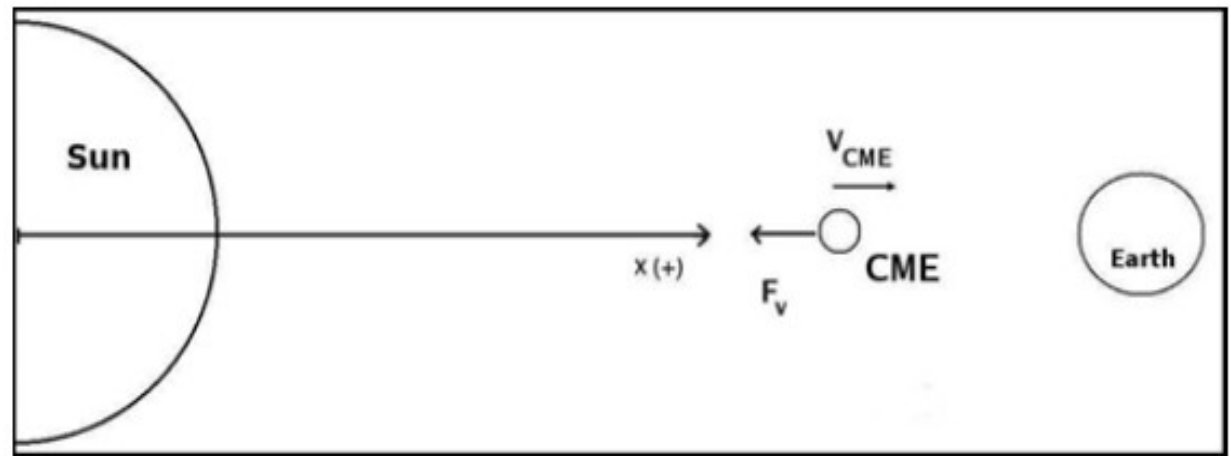
A subsets of CMEs show distinct quadratic-form correlations, of the form:

$$a = -k_2 (v - v_0) |v - v_0|$$

$k_2 =$  with  distance and width, $v_0 =$  with the distance.

acceleration-velocity relationship is interpreted as a **consequence of the aerodynamic drag**

The Drag Term



$$F_t = \frac{C_d A \rho U^2}{2}$$

$$F_l = 6\pi\mu RU$$

$$-\frac{T_1(U - U_{sw})^2}{2} = m_{cme} \frac{d(U - U_{sw})}{dt}$$

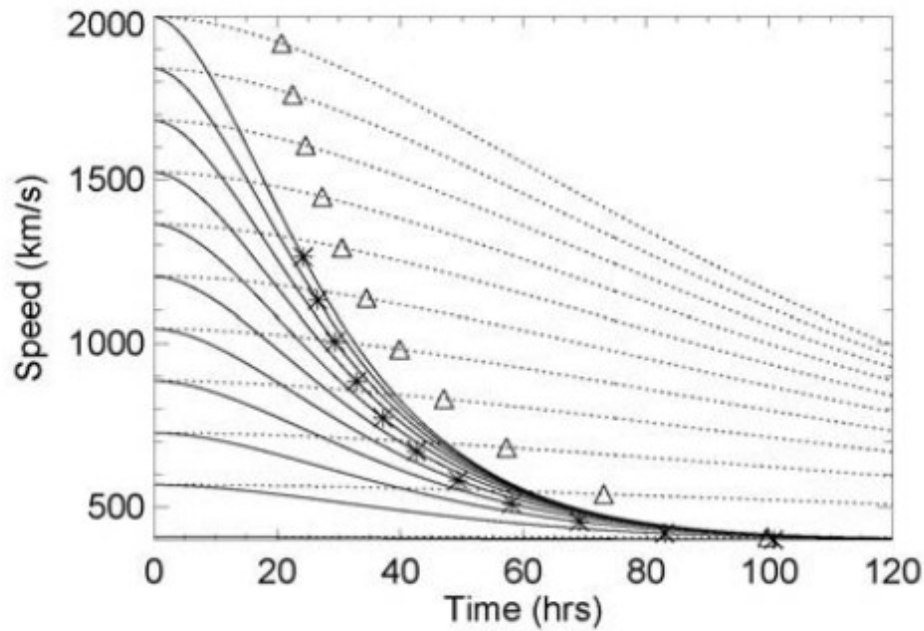
$$-L_1(U - U_{sw}) = m_{cme} \frac{d(U - U_{sw})}{dt}$$

U_{sw} = solar wind velocity,

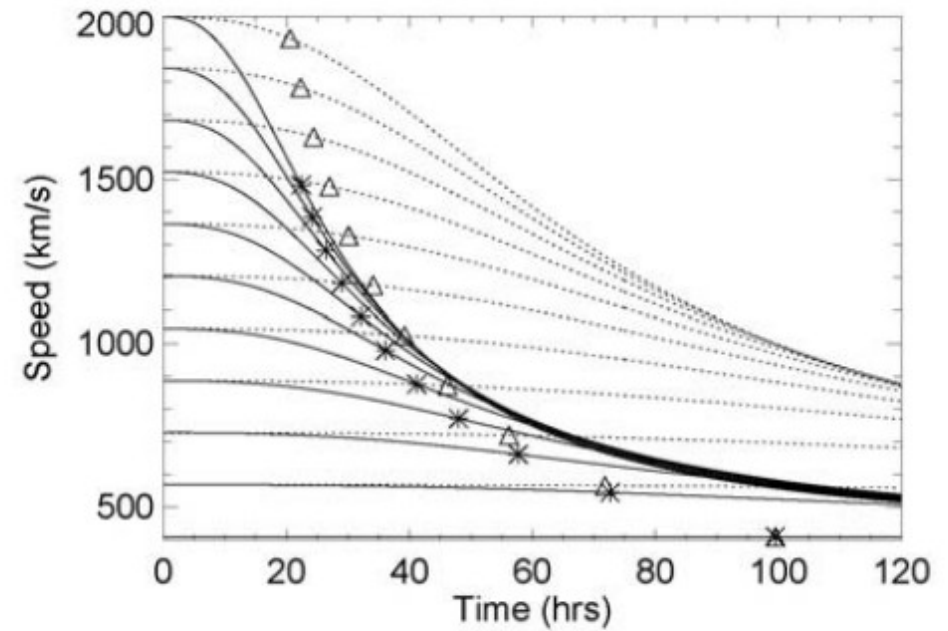
m_{cme} = mass CME

$$T_1 = C_d A \rho_{sw}$$

$$L_1 = 6\pi R \mu$$



(a)



(b)

Figure 15: - a) Evolution of the ICME speed in terms of the initial CME speed under the laminar drag force. The dotted lines correspond to a viscous coefficient of 0.002 kg/m.s and the continuous lines to 0.02 kg/m.s. The stars and triangles represent the travel time from the Sun to 1 AU. b) Temporal behavior of the ICME speed under a turbulent drag force. The dotted lines correspond to a drag coefficient of 200 and the continuous lines to a value of 2000.
SOURCE: Borgazzi et al. (2008)

Vrsnak et al. (2009)

$$a = -\gamma(v - w)|v - w|,$$

$$\gamma = c_d \frac{A\rho_w}{m},$$

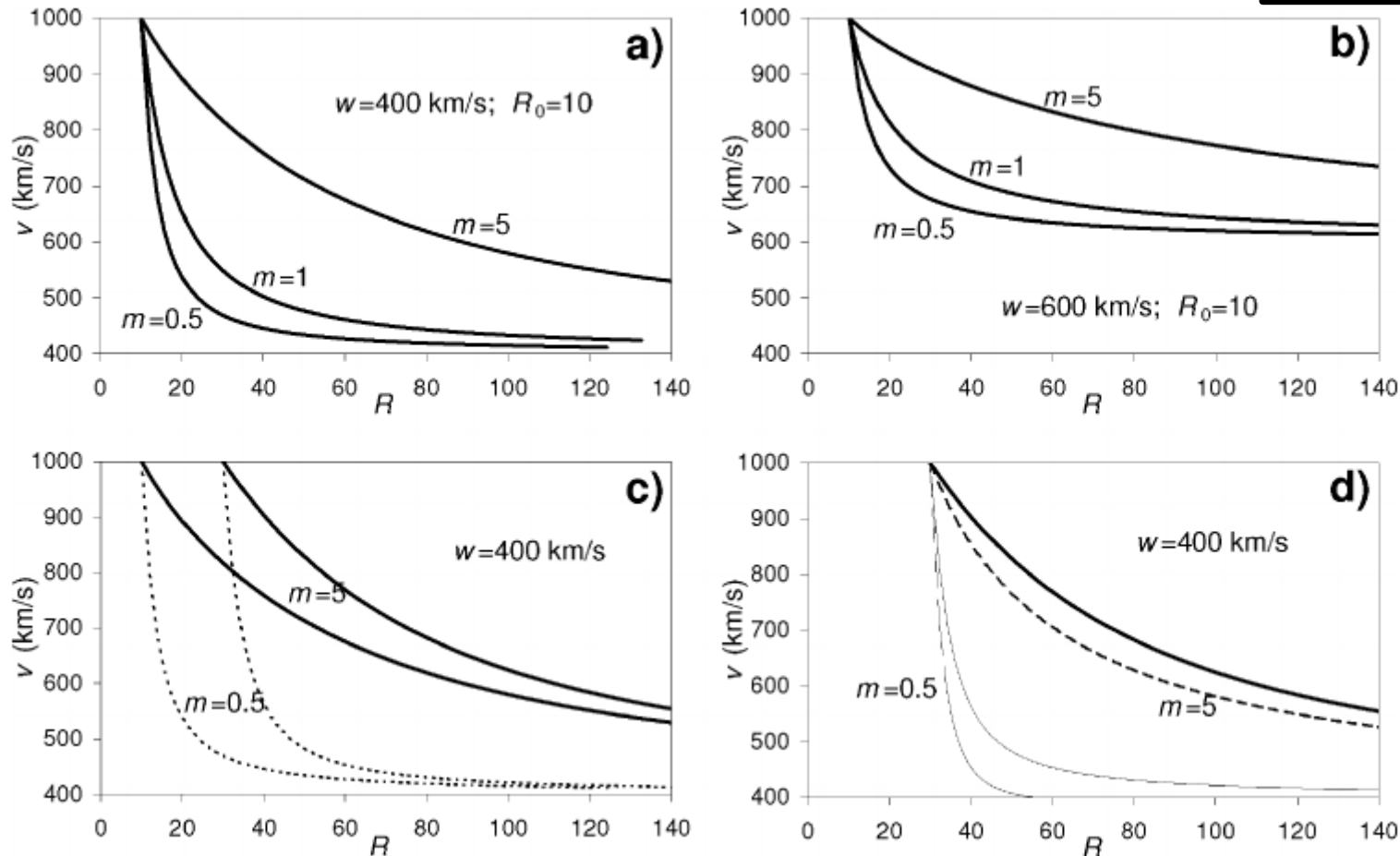


Figure 16: Calculated CME velocity as a function of the radial distance, which is expressed in units of the solar radius r_\odot . CME masses 'm' expressed in 10^{12} kg are written by the curves.

Variability of ICME radius

Solutions

$$-6\pi\mu x^p(U - U_{sw}) = m_{cme}U \frac{dU}{dx}$$

$$R = x^p$$

$$x^{(p+1)} - x_0^{(p+1)} = -\frac{m_{cme}(p+1)}{6\pi\mu} \left(U - U_0 + U_{sw} \ln \left[\frac{(U - U_{sw})}{(U_0 - U_{sw})} \right] \right)$$

$$-\frac{C_d\pi\rho_{sw}x^{2p}}{2}(U - U_{sw})^2 = m_{cme}U \frac{dU}{dx}$$

$$x^{(2p+1)} - x_0^{(2p+1)} = -2\frac{m_{cme}(2p+1)}{C_d\pi\rho_{sw}} \times \left[\frac{U_{sw}}{(U_0 - U_{sw})} - \frac{U_{sw}}{(U - U_{sw})} + \ln \left[\frac{(U - U_{sw})}{(U_0 - U_{sw})} \right] \right]$$

$$\nu = \frac{\mu}{\rho_{sw}}$$

viscosity

And if we use ...radius and density variable...we have: $\rho_{sw} = a/x^2$

$$R = x^p$$

$$-\frac{C_d \pi a x^{(2p-2)}}{2} (U - U_{sw})^2 = m_{cme} U \cdot \frac{dU}{dx},$$

Differential equation
(Turbulent case)

Solution

$$-\frac{C_d \pi a}{2 m_{cme} (2p-1)} [x^{(2p-1)} - x_0^{(2p-1)}] = \frac{U_{sw}}{(U_0 - U_{sw})} - \frac{U_{sw}}{(U - U_{sw})} + \ln \left[\frac{(U - U_{sw})}{(U_0 - U_{sw})} \right].$$

$$-6\pi\nu a x^{(p-2)} (U - U_{sw}) = m_{cme} U \cdot \frac{dU}{dx},$$

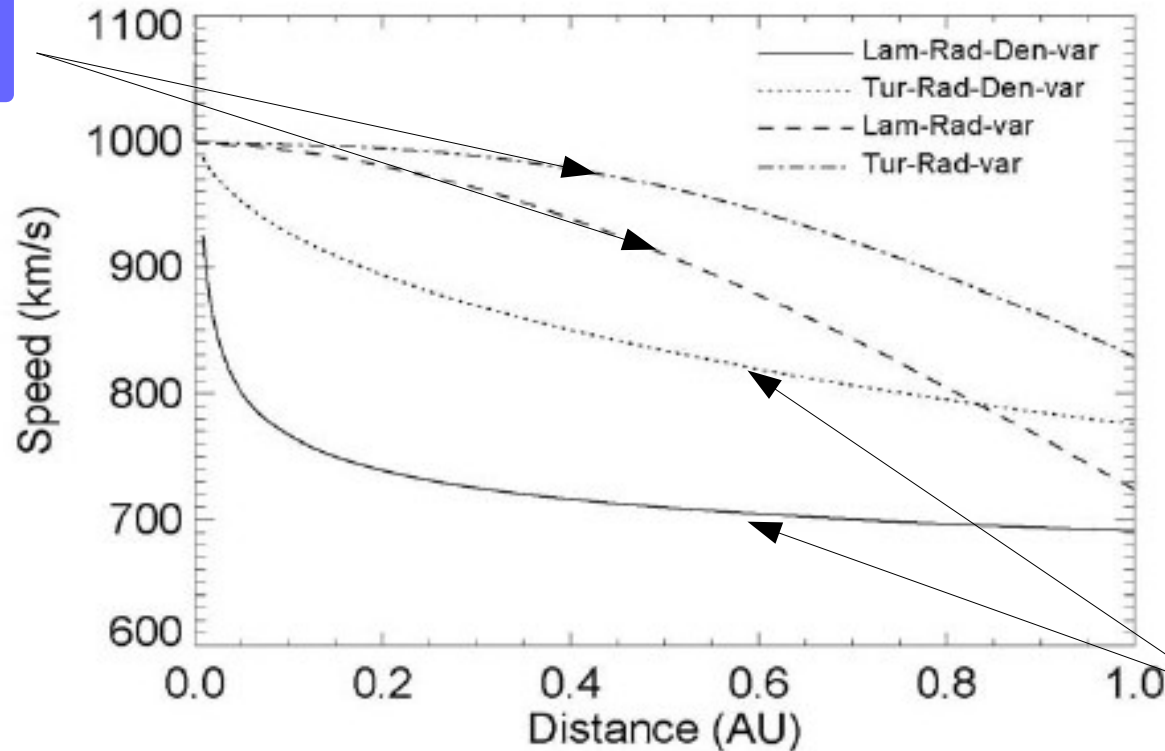
Differential equation
(Laminar case)

Solution

$$\nu = \frac{\mu}{\rho_{sw}}.$$

$$-\frac{6\pi\nu a}{m_{cme} (p-1)} [x^{p-1} - x_0^{p-1}] = U + U_{sw} \ln \frac{(U - U_{sw})}{(U_0 - U_{sw})} - U_0.$$

Rad-var



Rad-Den-var

FIGURE 6.20 - ICME speed versus distance for the four models analyzed in this work. a) laminar regime considering variability in ICME radius (Eq. 4.9) and $\mu = 0.175 \text{ g/cm}\cdot\text{s}$ (dashed line). b) turbulent regime considering variability in ICME radius (Eq. 4.10) and $C_d = 5 \times 10^4$ (dot-dashed line). c) laminar regime considering variability in ICME radius and SW density (Eq. 4.16) and $\nu = 8.75 \times 10^{20} \text{ cm}^2/\text{s}$ (continuous line). and d) turbulent regime considering variability in ICME radius and SW density (Eq. 4.13) and $C_d = 1.1 \times 10^5$ (dot line).

The result demonstrates that the Cargill et al. suggestion of a small drag coefficient near the Sun indeed eliminates the concave upward shape of the curve seen in the fixed C_D case.

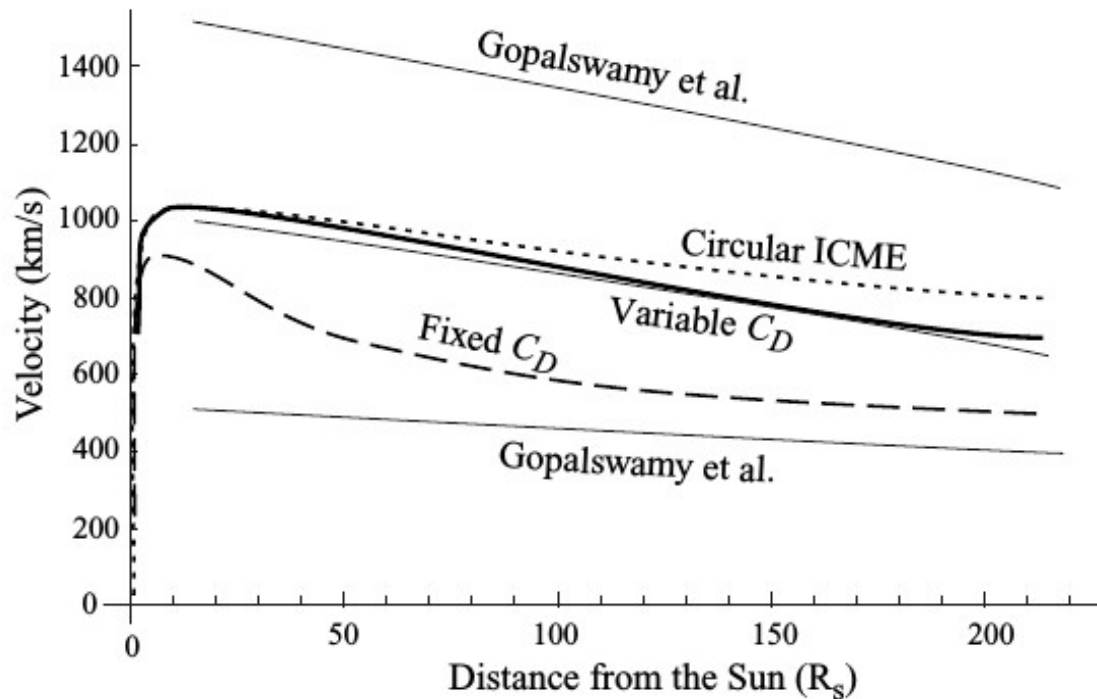


Figure 17: Velocity-versus-distance profiles showing three examples of the Gopalswamy et al. template.

- **Transit Time of Coronal Mass Ejections under Different Ambient Solar Wind Conditions**

Shanmugaraju and Vrsnak (2014)

Generally, the net force acting on the ICME can be written (Vršnak et al., 2006) as $\mathbf{F} = m(\mathbf{a}_L - \mathbf{a}_{drag} - \mathbf{g})$

- **CME propagation: where does the aerodynamic drag “take over”?**

Nishtha Sachdeva and Prasad Subramanian (2015)

$$F_{drag} = m_{cme} \frac{dV_{cme}}{dt} = -\frac{1}{2} C_D A_{cme} n m_p \left(V_{cme} - V_{sw} \right) \left| V_{cme} - V_{sw} \right|,$$

- **Predicting the arrival time of coronal mass ejections with the graduated cylindrical shell and drag force model**

Tong Shi , Yikang Wang , Linfeng Wan , Xin Cheng , Mingde Ding , and Jie Zhang, (2015)

$$\frac{dv}{dt} = -\gamma(v - w) |v - w|^{\beta-1}.$$

*Muchas gracias...
Thanks...*